Toroidal ion temperature gradientdriven weak turbulence

Nathan Mattor

Citation: Phys. Fluids B 3, 1913 (1991); doi: 10.1063/1.859660
View online: http://dx.doi.org/10.1063/1.859660
View Table of Contents: http://pop.aip.org/resource/1/PFBPEI/v3/i8
Published by the American Institute of Physics.

Toroidal ion temperature gradient-driven weak turbulence

Nathan Mattor[a)]
Culham Laboratory, Abingdon, Oxfordshire OX14 3DB, England

(Received 21 September 1990; accepted 1 April 1991)

In this paper, a theory of toroidal ion temperature gradient-driven weak turbulence near the threshold is presented. The model considers gyrokinetic ions and adiabatic electrons in toroidal geometry. The linear theory considers modes with $k_\theta \rho_i \sim O(1)$ (generally not considered in toroidal theories), giving a toroidal threshold regime dominated by transit resonances (as opposed to the more usually considered drift resonances), and with a stability threshold of $\eta_{\rm thresh}^{\rm tor} \simeq 1 + 2\epsilon_n [2/\tau + 1/(1+\hat{s})]$. It is shown that when $0 < \eta_i - \eta_{\rm thresh}^{\rm tor} < 2\sqrt{1+1/\tau} \times L_n/\sqrt{RL_T}$ then $0 < \gamma < \omega_r$, and a weak turbulence expansion can be used to treat the nonlinearity. The instability is saturated via nonlinear ion resonance, and it is shown that this nonlinear process transfers energy directly from the waves to the ion distribution function, and does not conserve wave energy. The saturated spectrum is calculated, and the resulting ion thermal conductivity is found to be $\chi_i = \sqrt{1+1/\tau}\,[(\eta_i - \eta_{\rm th}^{\rm tor})/\eta_i]\,(\sqrt{L_T}/R^{3/2})\rho_i^3 \Omega_i$, which is smaller than typical mixing length estimates by a factor of about L_T/R, but in the range of tokamak observations. The diffusive nature of the transport (requiring a short radial step size) is reconciled with the broad radial extent of the toroidally coupled linear modes by postulating that it is the nonlinear beat wave between linear modes (not the radial width of a single linear mode) that determines the step length appropriate for transport.

I. INTRODUCTION

The theory of ion temperature gradient-driven turbulence ("η_i turbulence") is able to explain many *qualitative* features of tokamak confinement,[1-3] but *quantitatively* the theory and local experimental measurements can sometimes differ by an order of magnitude.[4-7] However, the available theoretical predictions are generally based on rather idealized models, and several studies have shown that there can be significant quantitative corrections (orders of magnitude) coming from effects which are often neglected in the interest of analytical tractability. No theory to date has combined all such effects and produced a prediction of the transport, and so it can be argued that disagreements between existing theories and experiment are inconclusive. A more complete theory is required, and the present work is part of an effort to provide this.

The paradigm model of the η_i instability has generally been the slab fluid model. This mode is basically an ion sound wave parallel to the magnetic field, which accesses the free energy source of the radial ion temperature gradient.[8-10] Nonlinearly, this mode evolves to the strong turbulence regime, and gives rise to an ion thermal conductivity comparable to the mixing length level,[11-13] $\chi_i \sim \gamma/k_r^2$. Although this slab fluid model has been useful for exploring the qualitative behavior of the mode, the quantitative accuracy is uncertain at best. Threshold and toroidal effects can cause significant modifications to the predictions.

Near the threshold of the instability (often the regime of experimental interest), several features of the basic fluid η_i mode are altered. Linear ion resonances become important (occurring in the slab limit for particles with $\omega = k_\parallel v_\parallel$), and damp the mode,[8,11] so that the mode becomes fully stabilized when the density gradient becomes steeper than the ion temperature gradient (i.e., when $\eta_i \equiv d \ln T_i / d \ln n_0 \lesssim 1$). Nonlinear ion resonances (also known as nonlinear Landau damping or ion Compton scattering) accompany these linear resonances[14] and replace the fluid saturation mechanism (multiple wave resonance). Additionally, when the growth rate is smaller than the frequency, $\gamma < \omega_r$, the commonly used estimates from the strong turbulence ordering (such as the mixing length estimate) break down, and a wave kinetic formulation[15] is more appropriate. This threshold regime has been explored in Ref. 14 in slab geometry. Although the threshold regime covers only a certain range of η_i near the threshold, the results give insight into the behavior of nonlinear Landau damping, which can be expected to be important at higher values of η_i for modes of higher radial wave number (often denoted by l).

Toroidicity enters through the magnetic drift velocity, $\mathbf{v}_{Di}$, and also introduces several major changes in the basic picture. One change is the introduction of a new destabilization mechanism, coming from a pressure gradient in the presence of unfavorable toroidal curvature (analogous to the classical Rayleigh–Taylor instability), which competes with the sound wave destabilization mechanism of the basic instability. A second change is the introduction of toroidal coupling, which linearly joins modes with the same toroidal mode number n, and tends to make the modes a good deal broader radially. Toroidally coupled modes are generally described by a two-dimensional partial differential equation (PDE), which can be rendered tractable via introduction of the ballooning formalism.[16] Finally, the introduction of $\mathbf{v}_{Di}$ complicates the ion resonance condition, which becomes $\omega - k_\parallel v_\parallel - \mathbf{k}_\perp \cdot \mathbf{v}_{Di} = 0$, and thus acquires a quadratic de-

a) Present address: Center for Plasma Theory and Computation, University of Wisconsin, Madison, Wisconsin 53706.

 0899-8221/91/081913-14$02.00

pendence on both $v_\parallel$ and $v_\perp$.

The net effect of toroidicity on the η_i mode is not well established, since the literature contains a diversity of views. One such point is the relation between the toroidal (bad curvature) and slab (sound wave) destabilization mechanisms. Horton *et al.*[17] find that the character of the mode depends on the macroscopic geometry, namely, that when $2L_s < R$ the modes are slablike, changing over to a ballooninglike structure in the opposite limit. Guo *et al.*[18] find that the mode changes character depending on the regime in k space, such that toroidal destabilization dominates when $k_\theta \rho_i \ll L_T/R$, and becomes negligible in the opposite limit. (Although their study is nominally restricted to the regime $L_n \to \infty$, it appears that similar results can be obtained when this condition is relaxed.[19]) Other studies[20] use the term slab and toroidal "branches," implying a picture of two *coexisting* instabilities. A clearer picture of the relation between the slab and toroidal destabilization mechanisms is needed. A second point of uncertainty is whether parallel ($\omega \simeq k_\parallel v_\parallel$) or drift ($\omega \simeq \mathbf{k}_\perp \cdot \mathbf{v}_{Di}$) resonances (or neither) are important in the vicinity of the threshold. Various authors retain either the former[21] or the latter[19,22] and neglect the other, or neglect both,[23] but never with any apparent assessment of the relative magnitude. Although any of these techniques apparently produces roughly the same linear stability threshold, the transport (of concern in the present study) is more sensitive to the details of the dynamics, and so the resonance issue must be addressed. A third point of uncertainty is the determination of the radial width Δr of the toroidally coupled modes. The studies of Hastie *et al.*[24] and Connor and Taylor[25] find that the radial envelope of the linear modes is determined by terms that vary as $d^2\omega_{*i}/dr^2$. Since such terms are generally ignored in η_i mode theory, this implies $\Delta r = \infty$ to the order generally considered. Guo *et al.*[18] argue that when toroidal destabilization is subdominant, the modes are not toroidally coupled and the separation of rational surfaces can be used, $\Delta r \sim 1/k_\theta \hat{s}$. Biglari *et al.*[20] use the fact that the ballooning coordinate behaves like the Fourier conjugate to the radial coordinate to argue that $\Delta r = 1/k_\theta \hat{s} \Delta_{\hat{\theta}}$, where $\Delta_{\hat{\theta}}$ is the parallel width of the quasimode in ballooning space. Given this diversity of viewpoints, it is important to resolve the issue of what determines Δr, since the choice makes a significant difference on the scalings, magnitude, and underlying nature (diffusive or convective) of the resulting transport. Finally, Hirose and Ishihara[26] claim that toroidal effects completely stabilize the mode, which stands in contradiction to most other studies. In summary, the present understanding of the toroidal η_i mode can be characterized as having a number of diverging views with few studies attempting to bridge the gaps.

In this paper, we present a theory of weak toroidal η_i turbulence near the threshold of instability, thus combining the effects mentioned above (and in the process, new results emerge regarding both). The geometrical model consists of concentric circular flux surfaces, with radial gradients of density and ion temperature. Fluctuations are electrostatic, and described by the nonlinear ion gyrokinetic equation,[27] adiabatic electrons and quasineutrality. The ballooning formalism[16] is used to treat the toroidal mode structure. This complicated set of equations is rendered tractable by treating $\gamma/\omega_r < 1$ as a small parameter (where ω_r and γ are the linear frequency and linear growth rate, respectively). With this ordering, the lowest-order equation describes ω_r and the linear mode structure, and at first order is the wave kinetic equation, describing linear growth and nonlinear saturation of the modes. The condition $\gamma/\omega_r < 1$ defines the validity regime for the theory, which may be termed the "threshold regime." In the linear theory, transit resonances and sound wave dynamics (often neglected *a priori*) are retained via the "curvature approximation," and it is found that they can give the dominant contribution to the growth rate near the threshold (rather than the more usually considered drift resonances and curvature effects). A new method of solving the parallel mode equation is introduced, whereby asymptotically vanishing solutions are constructed by matching to the Bloch functions (also known as Floquet solutions). This produces different results from the more usual techniques. In the nonlinear theory, the wave kinetic equation is solved to yield the quasimode spectrum in both k_r and k_θ. The presence of different k_r in the spectrum is particularly important here, since interaction of modes with different k_r produces fluctuations with a small radial correlation length, consistent with diffusive radial transport (the linear modes have a radial correlation length that is essentially infinite). This point is discussed further in Sec. V.

The main results of this work are as follows.

(1) For η_i in the range $0 < \eta_i - \eta_{\text{thresh}}^{\text{tor}} < 2\sqrt{1 + 1/\tau} L_n/\sqrt{R L_T}$, the toroidal η_i mode is in the "threshold regime," characterized by weak turbulence and the prominence of ion resonances in the basic linear and nonlinear dynamics.

(2) Unstable toroidal modes are found for which sound wave destabilization (not unfavorable curvature) is the dominant drive. As a result, unstable linear modes can be located in regions of both good and bad curvature.

(3) The toroidal linear stability threshold is found to be

$$\eta_{\text{thresh}}^{\text{tor}} \simeq 1 + 2\epsilon_n [2/\tau + 1/(1 + \hat{s})],$$

where $\tau = T_e/T_i$, $\hat{s} = d \ln q / d \ln r$, and $\epsilon_n = L_n/R$.

(4) The mode saturates by nonlinear parallel Landau damping, whereby an ion resonates with the beat wave between two modes. Results indicate that this process transfers energy from the mode with lower $k_\parallel$ to the ions, so that turbulence energy is not conserved nonlinearly.

(5) The quasimode spectrum in the toroidal threshold regime is found to be[28]

$$\left| \frac{e\hat{\phi}_{\mathbf{k}}}{T_i} \right|^2 \simeq \frac{1}{(2\pi)^2} \frac{q}{r} \frac{\eta_i - \eta_c^{\text{tor}}(\mathbf{k})}{|\ln \partial\zeta/\partial\theta_{\mathbf{k}}|} \frac{1}{R^2 k_\theta^3},$$

and $|\hat{\phi}_{\mathbf{k}}^2| = 0$ in regions of k space, where $\eta_i \leqslant \eta_c^{\text{tor}}$. (The logarithmic factor in the denominator is regarded to be complicated, but with weak scalings and of order unity; here, $\zeta \equiv \omega_{\mathbf{k}}/\sqrt{2} k_\parallel v_{\text{th},i}$ and $\theta_{\mathbf{k}} \equiv k_r/k_\theta \hat{s}$, where $v_{\text{th},i}$ is the ion thermal velocity.) The spectrum is relatively flat in $\theta_{\mathbf{k}}$ (the index of the center of the quasimode), due to the growth rate having weaker dependence on $\theta_{\mathbf{k}}$ than on k_θ.

(6) The ion thermal conductivity in the threshold regime is

$$\chi_i = \sqrt{1+\frac{1}{\tau}}\left(\frac{\eta_i-\eta_{\rm th}^{\rm tor}}{\eta_i}\right)\frac{\sqrt{L_T}}{R^{3/2}}\rho_i^3\Omega_i,$$

which is less than the fluid regime value[29] by an approximate factor of L_T/R. It is found that the estimate $\chi_i \simeq \zeta^2\gamma/k_r^2$ is more appropriate than the mixing length estimate for the present case [where ζ is defined in item (5) above].

The remainder of this paper is organized as follows. In Sec. II we outline the basic model and equations. In Sec. III A, the linear mode equation is derived, and in Sec. III B this is solved to yield the frequency, growth rate, and basic mode structure in the neighborhood of the threshold. Section IV contains the nonlinear theory, including a weak turbulence derivation of the damping from nonlinear ion Landau resonances, and a calculation of the saturated spectrum. Section V contains a derivation of the ion thermal transport associated with the saturated spectrum, and Sec. VI is a summary and conclusions.

II. MODEL

The geometry of the toroidal η_i mode is described here by circular concentric toroidal flux surfaces, with radial gradients of density and ion temperature. The coordinate system is defined by the r (radial), θ (poloidal), and φ (toroidal) directions, oriented such that $\hat{r}\cdot(\hat{\theta}\times\hat{\varphi})=1$. The magnetic field is given by $\mathbf{B}=|B|\hat{b}$, where $|B|=B_0[1-(r/R)\cos\theta]$ and $\hat{b}=\hat{\varphi}+(B_\theta/B_\varphi)\hat{\theta}$.

With such a geometry, the toroidally coupled modes can be described by the ballooning representation,[16] whereby

$$\tilde{\phi}(\mathbf{x},t)=\int dk_r\sum_n\sum_m \exp[i(n\varphi-m\theta+k_r r)] \times\int_{-\infty}^{\infty} d\hat{\theta}\exp[i(m-nq)\hat{\theta}]\hat{\phi}_{\mathbf{k}}(r,\hat{\theta},t), \quad (1)$$

where the quasimode $\hat{\phi}_{\mathbf{k}}$ is required to vanish asymptotically in $\hat{\theta}$. Equation (1) represents $\tilde{\phi}(\mathbf{x})$ as a sum of Fourier modes, indexed with n, m, and k_r. It is also possible, by summing the modes of different m, to represent $\tilde{\phi}(\mathbf{x})$ as a sum of quasimodes, which have a structure that is extended radially and twists with the sheared field lines:

$$\tilde{\phi}(\mathbf{x},t)=2\pi\int dk_r\sum_n\sum_{p=-\infty}^{\infty}\exp\{i[n\varphi-nq(\theta+2\pi p) + k_r r]\}\hat{\phi}_{\mathbf{k}}(r,\theta+2\pi p,t). \quad (2)$$

Equations (1) and (2) are equivalent linearly, but in a random phase nonlinear theory it must be decided whether it is the Fourier modes or the quasimodes that acquire the random phase factor. For the present situation, note that the modes are in the weak turbulence regime, for which the linear and nonlinear mode structures are not appreciably different. Thus the turbulence must be represented as a sum of randomly phased *quasimodes*, since these are the correct linear modes, and a random phase is assigned to each n and k_r (although periodicity in θ dictates that modes with only p different have the same phase). It must be emphasized that there is no radial envelope for the quasimodes unless explicitly determined[24,25] from terms that vary as $d^2\omega_{*i}/dr^2$, which is not attempted here, nor apparently in any other analysis of the toroidal η_i mode. In the present model, a finite radial correlation length arises *nonlinearly* through the coexistence of modes with different k_r, a point developed further in Sec. V.

Fluctuations are electrostatic, and described by the nonadiabatic part of the ion distribution function, $\tilde{h}(\mathbf{x},\mathbf{v},t)$, and the electrostatic potential $\tilde{\phi}(\mathbf{x},t)$. It is assumed that fluctuations have perpendicular length scales much smaller than those of the equilibrium gradients, and time scales in the regime $v_i\sim\omega/k_\parallel\ll v_e$, so that ions are resonant and electrons are adiabatic. With these assumptions, the fields evolve by the nonlinear ion gyrokinetic equation written in the ballooning formalism[27]

$$\left(\frac{\partial}{\partial t}+v_\parallel\nabla_\parallel+i\omega_{Di}\right)\hat{h}_{\mathbf{k}}(\hat{\theta},\mathbf{v},t)-F_{\rm M}J_0(k_\perp v_\perp)\left(\frac{\partial}{\partial t}+i\omega_{*i}^T\right) \times\hat{\phi}_{\mathbf{k}}(\hat{\theta},t)=2\pi\sum_{p',p''}\sum_{n'+n''=n}\int dk_r'\,\hat{s}k_\theta' k_\theta'' \times[\theta_{\mathbf{k}'}-\theta_{\mathbf{k}''}+2\pi(p'-p'')]J_0(k_\perp' v_\perp) \times\hat{\phi}_{\mathbf{k}'}(\hat{\theta}-2\pi p',t)\hat{h}_{\mathbf{k}''}(\hat{\theta}-2\pi p'',\mathbf{v},t), \quad (3)$$

(with $k_r''=k_r-k_r'-2\pi p'k_\theta'-2\pi p''k_\theta''$ required for radial three wave matching), and the quasineutrality equation with adiabatic electrons:

$$\left(1+\frac{1}{\tau}\right)\hat{\phi}_{\mathbf{k}}(\hat{\theta},t)=\int d^3v\,J_0(k_\perp v_\perp)\hat{h}_{\mathbf{k}}(\hat{\theta},\mathbf{v},t). \quad (4)$$

Here $\hat{h}$ is the nonadiabatic part of the ion distribution function, $\hat{\phi}$ is the electrostatic potential normalized to e/T_i, $\hat{\theta}$ is the parallel coordinate in ballooning space, $k_\theta=nq/r$ is the poloidal wave vector, k_r is the absolute radial wave vector that indexes the quasimode, $\theta_{\mathbf{k}}=k_r/\hat{s}k_\theta$, $k_r(\hat{\theta})=k_\theta\hat{s}(\hat{\theta}-\theta_{\mathbf{k}})$ is the local radial wave vector, $k_\perp^2(\hat{\theta})$ is the square of the local perpendicular wave vector, $F_{\rm M}$ is a local Maxwellian with radial T_i and n gradients, J_0 is a Bessel function,

$$\omega_{Di}=\omega_{*i}\epsilon_n[\cos\hat{\theta}+\hat{s}(\hat{\theta}-\theta_{\mathbf{k}})\sin\hat{\theta}](v_\parallel^2+v_\perp^2/2),$$

$\omega_{*i}^T=\omega_{*i}[1-\eta_i(3-v^2)/2]$, $\omega_{*i}=-k_\theta\rho_i^2\Omega_i/L_n$, $\eta_i=L_n/L_{T_i}$, $L_n^{-1}=-d\ln n/dr$, $L_T^{-1}=-d\ln T/dr$, $\hat{s}=d\ln q/d\ln r$, q is the safety factor, $\tau=T_e/T_i$, $\epsilon_n=L_n/R$, $\epsilon_T=L_T/R$, R is the major radius, $v_i^2=T_i/m_i$, $\Omega_i=eB/m\_c$, $\rho_i=v_i/\Omega_i$, and distance and time have been undimensionalized to ρ_i and $1/\Omega_i$.

III. LINEAR THEORY

Although the linear theory of the toroidal η_i mode has been examined previously by several authors,[19,21–23] these studies have been concerned only with the linear stability threshold. Here, a more detailed linear theory must be undertaken, in order to obtain the information necessary to resolve nonlinear saturation and transport. One issue is whether drift or parallel resonances are more important in this regime. The uncertainty arises because the velocity

space integral, Eq. (5) below, is difficult to perform while keeping both resonances, and so the general approach has been to retain one and expand the other, making assessment of the relative contributions difficult. It appears that whichever expansion is performed, the linear threshold is insensitive (crudely speaking) and varies as $\eta_c^{\rm tor} \sim 1 + O(L_n/R)$, but the nonlinear resonances considered in Sec. IV may be more sensitive to the resonance type. Other issues that need resolution in the linear theory are the value of k_r (since this determines the radial correlation length for transport), the parallel mode structure (which determines k_r), and the ordering of ω_r, γ, $k_\parallel$, and k_θ for the unstable modes.

A. Linear mode equation

The parallel structure of the toroidal η_i modes may be described by an integral equation in $\hat{\theta}$,[19] but such a formulation tends to be analytically intractable and is abandoned here. Instead the parallel dynamics are described semilocally, meaning that $\nabla_\parallel$ is used interchangeably with $ik_\parallel = i\hat{k}_{\hat{\theta}}/qR$, which is then treated as a number and not as an operator (consistent with a WKB description of the mode structure). (Here $\hat{k}_{\hat{\theta}}$ represents the dimensionless wave number in the ballooning angle, and is not to be confused with the poloidal wave number $k_\theta \equiv nq/r$.) Such a description applies when the solution has a shorter scale length than the coefficients in the equation, which can be verified *a posteriori* here. With this, the linearized version of Eq. (3) can be solved by Fourier transforming in t and substituting $\hat{h}_{\rm k}$ into Eq. (4) producing

$$\left(1+\frac{1}{\tau}\right)\hat{\phi}_{\rm k} = \int d^3v \frac{\omega-\omega_*^T}{\omega - k_\parallel v_\parallel - \omega_{Di}} J_0^2(k_\perp v_\perp) F_{\rm M} \hat{\phi}_{\rm k}. \tag{5}$$

The usual way to examine the toroidal η_i threshold is (a) to expand the demominator in Eq. (5) for $k_\parallel v_\parallel < \omega_{Di}$ in order to perform the velocity integral, and then (b) to assume that the mode is localized to the bad curvature region, which requires that $k_\parallel \gtrsim 1/qR$. However, it appears that these two steps are in conflict (at least from the viewpoint of the local approach), since for both inequalities to be possible the condition $[\cos\hat{\theta} + \hat{s}(\hat{\theta}-\theta_{\rm k})\sin\hat{\theta}\,]\rho_i k_\theta (v_\parallel^2 + v_\perp^2/2)/v_\parallel \gg 1$ must be satisfied, which is not true, except over a small region of velocity space. Therefore this approach is abandoned here. Instead, the velocity space integral is performed (with a minimum of *a priori* ordering assumptions) via the "curvature approximation," made by substituting $v_\perp^2 \to 2v_\parallel^2$ in ω_{Di}. This choice is substitution is motivated by the fact that both quantities have the same mean value, and can be expected to have roughly the same general behavior. Quantitative accuracy of the curvature approximation is discussed by Terry *et al.*[22] With this, the velocity integral in Eq. (5) can be performed, producing

$$\epsilon_{\rm k}(\omega)\hat{\phi}_{\rm k}(\hat{\theta}) = 0, \tag{6}$$

where

$$\epsilon_{\rm k}(\omega) = 1 + \frac{1}{\tau} + \frac{\Gamma_0[k_\perp^2(\hat{\theta})]}{(a_+ - a_-)A}\left[\frac{\eta_i}{2}\left[a_+ Z'(a_+) - a_- Z'(a_-)\right] + \left(\frac{\eta_i}{\eta_c} - 1 + \Omega\right) \times \left[Z(a_+) - Z(a_-)\right]\right], \tag{7}$$

and

$$a_\pm = -\frac{\Omega}{2\zeta A} \pm \sqrt{\frac{\Omega^2}{4\zeta^2 A^2} + \frac{\Omega}{A}},$$

and $\eta_c^{-1} = \frac{1}{2} + b(1 - \Gamma_1/\Gamma_0)$ is the $k_\perp$-dependent threshold in the local slab theory,[10] Z is the plasma dispersion function, $\Gamma_n(b) = e^{-b} I_n(b)$, I_n is the modified Bessel function, $A = 4\epsilon_n[\cos\hat{\theta} + \hat{s}(\hat{\theta}-\theta_{\rm k})\sin\hat{\theta}\,]$, $\zeta = \omega/\sqrt{2}k_\parallel$, and $\Omega = \omega/\omega_{*,i}$. Equations (6) and (7) retain both slab and toroidal effects and apply to all relevant regimes of $k_\perp$, and so are well suited for a very general examination of the toroidal η_i threshold.

When $\epsilon_n \ll 1$ and $\eta_i - \eta_c < O(\sqrt{\epsilon_n})$, then Eq. (6) admits solutions with the ordering scheme $\zeta \sim \sqrt{\epsilon_n}$; $\Omega_I < \Omega_R \sim \epsilon_n$ (where $\Omega = \Omega_R + i\Omega_I$), $qRk_\parallel \sim 1/\sqrt{\epsilon_n}$, and $b_\theta \gtrsim 1$ (verifiable *a posteriori*). This solution also applies to flat density profiles, and for any of the following equations it is legitimate to take $L_n \to \infty$, as long as $\epsilon_T = L_T/R \ll 1$ still holds. Note that with this ordering, the dominant resonances are $\omega = k_\parallel v_\parallel$. It is possible that there is an alternative ordering in which the drift resonance dominates, but we have not been able to find such a solution to Eqs. (6) and (7). Expanding $a_\pm$ and $Z(a_\pm)$ with this ordering, $\epsilon_{\rm k}$ becomes

$$\epsilon_{\rm k}(\omega) = 1 + \frac{1}{\tau} + \frac{\Gamma_0[k_\perp^2(\hat{\theta})]\zeta}{\Omega}\left[\frac{\zeta\eta_i}{\Omega}(A-\Omega) + i\sqrt{\pi}\frac{k_\parallel}{|k_\parallel|}\left(\frac{\eta_i}{\eta_c} - 1 + \Omega - \eta_i\zeta^2\right)\right]. \tag{8}$$

This can be converted into a differential equation by rewriting $k_\parallel^2$ as $-(qR)^{-2}\partial^2/\partial\hat{\theta}^2$, and with this Eqs. (6) and (7) become

$$\frac{\partial^2}{\partial\hat{\theta}^2}\hat{\phi}_{\rm k} + Q(\Omega)\hat{\phi}_{\rm k} = 0, \tag{9}$$

where the "potential function" is given by

$$Q(\Omega) = -\frac{b_\theta q^2 \eta_i \Gamma_0[k_\perp^2(\hat{\theta})]}{2\epsilon_n^2(1+1/\tau)}\left[\frac{A}{2} - \Omega + i\frac{\sqrt{\pi}\Omega}{\zeta\eta_i}\left(\frac{\eta_i}{\eta_c} - 1 + \Omega - \eta_i\zeta^2\right)\right].$$

Equation (9) describes the frequency, growth rate, and parallel mode structure of the linear modes under the above ordering scheme. Note that Q depends on $\partial/\partial\hat{\theta}$ through the presence of $\zeta(k_\parallel)$, so that formally Eq. (9) is a third-order differential equation. However, such dependence only appears in terms that will be taken as higher order, and thus will be iteratively substituted from the lowest-order solution. The rest of this section is devoted to the solution of Eq. (9).

B. Linear modes

In this subsection we describe the solution of Eq. (9). Since the methods used are not standard, the first part is devoted to describing the analytical techniques used; the remainder examines the modes at high and low parallel mode number.

1. Method of solution

Equation (9) can be solved by taking $\lambda \sim \Omega_I/\Omega_R \ll 1$ (where $\Omega = \Omega_R + i\Omega_I$) as an ordering parameter (valid when η_i is sufficiently close to the threshold) and expanding $\hat{\phi} = \hat{\phi}^{(0)} + \lambda\hat{\phi}^{(1)}$ and $Q(\Omega) = Q_R(\Omega_R) + i\lambda\,[Q_I(\Omega_R) + \Omega_I\,\partial Q_R(\Omega_R)/\partial\Omega_R]$. This allows a perturbation solution for the mode structure, frequency (lowest order), and growth rate (next order).

The frequency Ω_R and the mode structure are described by Eq. (9) to lowest order in Ω_I/Ω_R, which is

$$\frac{\partial^2}{\partial\hat{\theta}^2}\hat{\phi}_k^{(0)} + Q_R(\Omega_R)\hat{\phi}_k^{(0)} = 0, \tag{10}$$

where

$$Q_R(\Omega_R) = -\frac{b_\theta q^2 \eta_i \Gamma_0[k_\perp^2(\hat{\theta})]}{\epsilon_n(1+1/\tau)} \times\left(\cos\hat{\theta} + \hat{s}(\hat{\theta}-\theta_k)\sin\hat{\theta} - \frac{\Omega_R}{2\epsilon_n}\right),$$

with the boundary condition that $\hat{\phi}_k^{(0)} \to 0$ as $\hat{\theta} \to \pm\infty$. The WKB solution of Eq. (10) is complicated by the fact that Q_R has an infinite number of turning points at intervals of about π. This means that the usual decaying WKB branch, $\hat{\phi} = \exp(-|\int_{\theta_T}^{\hat{\theta}}\sqrt{Q}\,d\hat{\theta}|)$, will pick up a component of the growing branch at each turning point, and thus not satisfy the boundary conditions. Instead, asymptotically vanishing solutions to Eq. (10) can be found in the regions in which $|\hat{\theta}-\theta_k| > \max[1,\Omega/2\epsilon_n]/\hat{s}$, in which case the term with $\sin\hat{\theta}$ dominates the potential and $\Gamma_0[k_\perp^2(\hat{\theta})] \simeq \Gamma_0(k_\theta^2)/\hat{s}|\hat{\theta}-\theta_k|$, and $Q_R(\hat{\theta})$ becomes

$$Q_R \simeq -\mu\,\mathrm{sgn}(\hat{\theta}-\theta_k)\sin\hat{\theta}, \tag{11}$$

where $\mu = b_\theta q^2\eta_i/\epsilon_n p$, and $p = (1+1/\tau)/\Gamma_0(k_\theta^2)$. Since Eq. (11) represents a periodic potential, then the vanishing eigenmodes are the Bloch functions,[30] for which $\hat{\phi}$ has the form $\exp(\alpha\hat{\theta})f(\hat{\theta})$, where f is a function with period 2π (further described in the Appendix). Between these two asymptotic regions is a "central region," defined as the region where Q_R is significantly different from Eq. (11). The central region is roughly where $|\hat{\theta}-\theta_k| < \max[1,\Omega/2\epsilon_n]/\hat{s}$, which will be taken as the average domain of the central region (although the boundary is difficult to define exactly). A normal mode extends between the two turning points bordering the central region, and will connect the two asymptotically decaying branches if the following phase quantization condition is satisfied (see the Appendix for a derivation):

$$\int_{\theta_{-Tc}}^{\theta_{+Tc}} \sqrt{Q_R(\Omega_R)}\,d\hat{\theta} = \pi l, \tag{12}$$

where $\theta_{\pm Tc}$ are the turning points bordering the "classically forbidden regions" on either side of the central region [i.e., $Q_R(\theta_{\pm Tc}) = 0$ and $Q_R(\theta_{\pm Tc} \pm \epsilon) < 0$], and l is a non-negative integer. As for the structure of the mode within the central zone, when $Q_R > 0$ the WKB solution for $\hat{\phi}^{(0)}$ is, up to a phase,

$$\hat{\phi}^{(0)} \simeq \sin\frac{[\int\sqrt{Q_R}\,d\hat{\theta}]}{Q_R^{1/4}}. \tag{13}$$

Figure 1 shows a shooting code solution of the $l = 4$ mode, showing the localization of the mode to the central region and decay outside this. For some modes, there will be parts of the central zone where $Q_R < 0$ (making $\hat{\phi}_k^{(0)}$ exponential in $\hat{\theta}$), but these regions will be less prevalent than the oscillatory regions described by Eq. (13). This is because (a) the tendency for $\Omega_R > 0$ (propagation in the ion diamagnetic drift direction) has the effect of making Q_R positive over the majority of the central region, and (b) every exponential solution must be matched on either side to an oscillatory solution of the form in Eq. (13), so that the amplitude in a given exponential zone will less than that of the neighboring oscillatory zone.

The growth rate is obtained from taking Eq. (9) to first order, which is

$$\left(\frac{\partial^2}{\partial\hat{\theta}^2} + Q_R\right)\hat{\phi}^{(1)} + i\left(Q_I + \Omega_I\frac{\partial Q_R}{\partial\Omega_R}\right)\hat{\phi}^{(0)} = 0, \tag{14}$$

where

$$Q_I = -(\mu\Omega_R/2\epsilon_n\eta_i\zeta)Z_i(\zeta)(\eta_i/\eta_c - 1 + \Omega_r - \eta_i\zeta^2), \tag{15}$$

and $Z_i = \sqrt{\pi}e^{-\zeta^2}k_\parallel/|k_\parallel|$. Multiplying Eq. (14) by $\hat{\phi}_k^{(0)}$, and taking $\int_{-\infty}^{\infty}d\hat{\theta}$ annihilates the $\hat{\phi}^{(1)}$ terms, and yields the following expression for the growth rate:

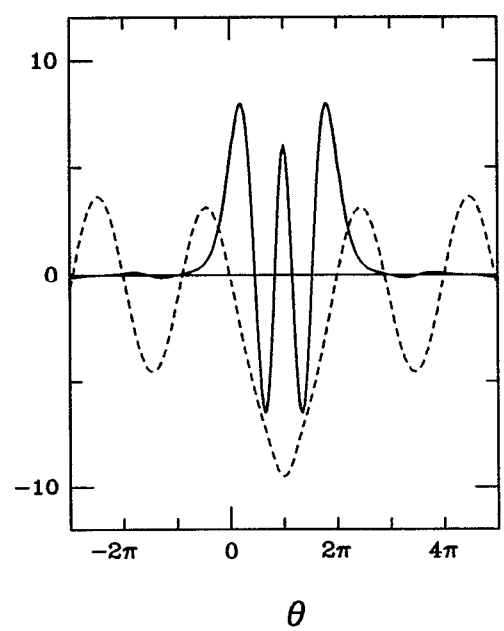

FIG. 1. Typical solution to Eq. (10), showing the potential, $-Q_R$ (dashed line), and the solution, $\hat{\phi}$ (solid line). Here $l = 4$, $\Omega_R = 0.103$, $b = 1$, $\epsilon_n = 0.5$, $\theta_k = \pi$, $q = 1$, $\eta_i = 1$, $\hat{s} = 1$, and $\tau = 1$.

$$\Omega_I = \frac{-\int_{-\infty}^{\infty} d\hat{\theta}\, Q_I(\Omega_R)(\hat{\phi}^{(0)})^2}{\int_{-\infty}^{\infty} d\hat{\theta}\,[\partial Q_R(\Omega_R)/\partial\Omega_R](\hat{\phi}^{(0)})^2}. \tag{16}$$

The threshold at a given $\mathbf{k}$, denoted as $\eta_c^{\rm tor}(\mathbf{k})$, can be estimated directly from Eq. (16) (without the need to calculate Ω_I first) by setting the numerator to zero, which produces

$$\eta_c^{\rm tor}(\mathbf{k}) \simeq \eta_c \frac{\int_{-\infty}^{\infty} d\hat{\theta}(1-\Omega_R+\eta_i\zeta^2)(\hat{\phi}^{(0)})^2/\zeta}{\int_{-\infty}^{\infty} d\hat{\theta}(\hat{\phi}^{(0)})^2/\zeta}, \tag{17}$$

where $\eta_c(k_\perp)\simeq\eta_c(k_\theta)$ has been used, valid for $k_\theta \gtrsim 1$. Equation (17) can be simplified by (a) approximating $\hat{\phi}$ by Eq. (13), with a width of $\Delta_{\hat{\theta}}$, (b) using the WKB approximation for $k_\parallel$, so that $k_\parallel^2 = Q_R/q^2R^2$, and (c) noting that $\hat{\phi}(\hat{\theta})$ oscillates much faster than $Q(\hat{\theta})$, so that the $\sin^2(\hat{k}_{\hat{\theta}}\hat{\theta})$ term coming from $(\phi^{(0)})^2$ can be replaced with $\frac{1}{2}$. These approximations produce

$$\eta_c^{\rm tor}(\mathbf{k}) \simeq \eta_c\left[1+\frac{\Omega_R}{2\Delta_{\hat{\theta}}}\int_{\theta_k-\Delta_{\hat{\theta}}}^{\theta_k+\Delta_{\hat{\theta}}} d\hat{\theta}\left(\frac{\Omega_R}{2\epsilon_n}\frac{p}{Q_R/\mu}-1\right)\right]. \tag{18}$$

Thus we have methods for evaluating $\phi^{(0)}(\hat{\theta})$, Ω_R, and Ω_I. The radial envelope of the linear modes is described by a higher-order equation in $d^2\omega_{*i}/dr^2$, but such detail is not necessary here, where radial structure is introduced nonlinearly (see the second paragraph of Sec. V).

2. High l limit

When l is high enough, $\Omega/2\epsilon_n$ is the dominant term in Q_R over most of the central region. In this limit, the phase quantization integral in Eq. (12) may be estimated by taking $Q_R \simeq \mu\Omega_R/2\epsilon_n$ and $\theta_{\pm Tc} \simeq \theta_k \pm \Omega_R/2\epsilon_n\hat{s}$ [obtained from Eq. (10) by balancing the $\sin\hat{\theta}$ and Ω_R terms]. This yields

$$\Omega_R \simeq 2\epsilon_n(\hat{s}^2l^2/\mu)^{1/3}. \tag{19}$$

Equation (19) can be compared with the shooting code trace of Ω_R vs k_θ shown in Fig. 2. In order to satisfy the assumption $\Omega_R/2\epsilon_n \gg 1$, Eq. (19) leads to the condition that $l \gg \sqrt{\mu}/\hat{s} \sim O(1/\sqrt{\epsilon_n})$. The high l modes extend across the central region, decaying exponentially outside this, and thus are centered around $\hat{\theta}=\theta_k$, with a width of approximately $(l^2/\mu\hat{s})^{1/3}$. Within this width, $\hat{\phi}^{(0)} \simeq \sin(\hat{k}_{\hat{\theta}}\hat{\theta})$, where $\hat{k}_{\hat{\theta}}^2 \simeq \mu\Omega_R/2\epsilon_n$.

The growth rate can be evaluated using Eq. (16), taking $Q_R \simeq \mu\Omega_R/2\epsilon_n$ across the width of $\phi^{(0)}$. This yields a linear growth rate of

$$\Omega_I \simeq \sqrt{\frac{\pi\epsilon_T}{p}}\left(\frac{\hat{s}^2l^2}{\mu}\right)^{1/6} \times\left[\frac{\eta_i}{\eta_c}-1-2\epsilon_n(p-1)\left(\frac{\hat{s}^2l^2}{\mu}\right)^{1/3}\right]. \tag{20}$$

Equation (20) shows that $\eta_c^{\rm tor}$ decreases with l, implying that the low l limit is the most relevant in the threshold regime.

3. Low l limit

Since, from above, only the lowest l are unstable near the threshold, it is important to note that the lower limit of l is

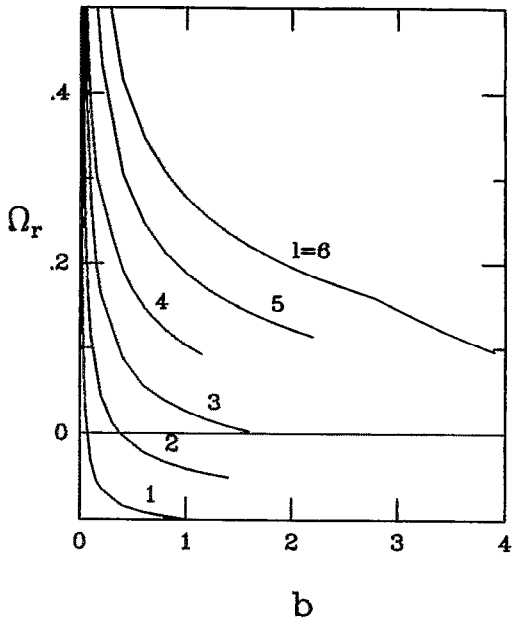

FIG. 2. The frequency Ω_R as a function of $b = k_\theta^2$, showing the complicated and dispersive nature of the dispersion relation. Here $b=1$, $\epsilon_n = 0.5$, $\theta_k = \pi, q = 1, \eta_i = 1, \hat{s} = 1$, and $\tau = 1$. Note that the termination of lower l branches with increasing b is a real physical effect, as discussed in Sec. III B 3. The apparent divergence of Ω_R as $b\to 0$ is a by-product of the standard ω/ω_{*i} normalization, and also the ordering $k_\theta\rho_i \gtrsim 1$ breaks down at some point before this limit.

$l \gtrsim \mu/\hat{s}$, not zero, as is often the case. To see this, note that as l decreases from the high l limit considered above, so also do the frequency Ω_R, the wave number, $\hat{k}_{\hat{\theta}}^2 \sim Q_R \sim \mu\max[1,\Omega/2\epsilon_n]$, and the mode width, $\Delta_{\hat{\theta}} \simeq \max[1,\Omega_R/2\epsilon_n]/\hat{s}$. This continues until $\Delta_{\hat{\theta}}$ and $\hat{k}_{\hat{\theta}}$ reach their lower limits of $\Delta_{\hat{\theta}} \sim 1/\hat{s}$ and $\hat{k}_{\hat{\theta}} \sim \sqrt{\mu}$. At this point l, which must obey the relation $l = \hat{k}_{\hat{\theta}}\Delta_{\hat{\theta}}$, cannot decrease further, and so $l \gtrsim \mu/\hat{s}$.

Unfortunately, the low l modes are difficult to treat analytically, since they have $\Omega_R/2\epsilon_n \sim \cos\hat{\theta} \sim 1$, so that Q_R cannot be easily ordered. However, the following general observations can be made.

(1) The real part of the frequency is determined by the phase quantization condition

$$\int_{\theta_k-1/\hat{s}}^{\theta_k+1/\hat{s}} d\hat{\theta}\sqrt{\frac{\Omega_R}{2\epsilon_n}-\cos\hat{\theta}} = \frac{\pi l}{\sqrt{\mu}}.$$

The solution of this involves inversion of an elliptic integral of the second kind, but the general features of the solution can be obtained by considering the case, where l is just above its lower cutoff. In this case the solution can be found by expanding the radical for $\Omega_R/2\epsilon_n > \cos\hat{\theta}$, performing the integral, and solving by iteration, which produces

$$\frac{\Omega_R}{2\epsilon_n} \simeq \left(\frac{\hat{s}\pi l}{2\sqrt{\mu}}\right)^2 + \frac{\sqrt{\mu}}{\hat{s}\pi l}\hat{s}\sin\left(\frac{1}{\hat{s}}\right)\cos\theta_k.$$

For higher l, the first term dominates, but as l decreases to its lower limit of $\sqrt{\mu}/\hat{s}$ then both terms become of order 1, after

which the mode is cut off. The cutoff point is difficult to determine analytically, and the value of Ω_R at this point is complicated by the quantization of l, but it is sufficient for the present purposes to characterize the frequency of these lowest l modes as

$$\Omega_r \simeq 2\epsilon_n \pm O(\epsilon_n). \tag{21}$$

This value and the high level of dispersiveness are verified by shooting code solutions to Eq. (10). (Figure 2 shows a typical numerical dispersion curve. Note that the termination of lower l branches with increasing b is a real physical effect. The apparent divergence of Ω_r as $b \to 0$ is a by-product of the standard $\omega/\omega_{*,i}$ normalization, and also the ordering $k_\theta \rho_i \gtrsim 1$ breaks down at some point before this limit.)

(2) The modes cover the central zone, and thus are centered around $\hat{\theta} = \theta_k$, with a width of about $1/\hat{s}$ (with an additional width of up to π, from the fact that the neighboring turning points might not be at precisely $\theta_k \pm 1/\hat{s}$. The parallel wavelength $\hat{k}_{\hat{\theta}}$ from the WKB approximation, is approximately $\hat{k}_{\hat{\theta}} \simeq \sqrt{\mu}$. Thus $\hat{\phi}$ can be approximated as

$$\hat{\phi}(\hat{\theta}) \simeq \sin(\sqrt{\mu}\hat{\theta})\Theta(-|\hat{\theta} - \theta_k| + 1/\hat{s}), \tag{22}$$

where Θ is the Heaviside step function, $\mu = b_\theta q^2 \eta_i / \epsilon_n p$, and $p = (1 + 1/\tau)/\Gamma_0(k_\theta^2)$.

(3) The value of η_c^{tor} can be obtained from Eq. (18), noting that the $\sin \hat{\theta}$ term is small in the central region,

$$\eta_c^{\text{tor}}(\mathbf{k}) \simeq \eta_c(b_\theta)\left[1 + \Omega_R \frac{\hat{s}}{2} \times \int_{\theta_k - \hat{s}}^{\theta_k + \hat{s}} d\hat{\theta}\left(\frac{p}{1 - 2\epsilon_n \cos\hat{\theta}/\Omega_R} - 1\right)\right]. \tag{23}$$

The qualitative behavior of η_c^{tor} can be assessed by taking $\Omega_R/2\epsilon_n \to 1$ and expanding the integrand for $|\cos\hat{\theta}| < 1$ (valid for most $\hat{\theta}$), which yields

$$\eta_c^{\text{tor}}(\mathbf{k}) \simeq \eta_c(b_\theta)\{1 + 2\epsilon_n[(p-1) + \hat{s}\sin(1/\hat{s})\cos\theta_k]\}. \tag{24}$$

This is minimized at about $b_\theta \sim 1$ (for $b_\theta \to 0$, η_c increases from 1 to 2, and for $b_\theta > 1$, η_c stays constant, but p increases proportional to k_θ) and $\theta_k = 0$ or π (depending on the sign of $\sin 1/\hat{s}$), giving the following approximation for the absolute stability threshold denoted $\eta_{\text{thresh}}^{\text{tor}}$:

$$\eta_{\text{thresh}}^{\text{tor}} \simeq 1 + 2\epsilon_n[2/\tau + 1/(1 + \hat{s})]. \tag{25}$$

(4) The wave number regime of the unstable modes near threshold is $k_\theta \rho_i \sim 1$, parallel wave number (in real space) $k_\parallel \sim k_\theta \rho_i \sqrt{\tau\Gamma_0/(1+\tau)RL_{T_i}}$, and k_r such that mode centers are distributed poloidally in a complicated manner, though assumedly with a fairly even poloidal distribution, since the curvature effects do not contribute directly to the growth rate. One should note that k_r refers here to the index of the center of the quasimode through the relation $\theta_k = k_r/k_\theta \hat{s}$; in terms of a radial Fourier decomposition, $k_r^{\text{Fourier}} \sim k_\theta \hat{s} \Delta_{\hat{\theta}} \simeq k_\theta$. Thus the linear modes have rough r-θ isotropization, even though the ballooning representation treats these two dimensions quite differently!

(5) The growth rate, from Eq. (16), is given roughly by

$$\Omega_I \simeq \sqrt{\epsilon_T/(1 + 1/\tau)}\,(1/k_\theta \eta_c)[\eta_i - \eta_c^{\text{tor}}(\mathbf{k})]. \tag{26}$$

The preceding linear theory only roughly represents the complicated behavior of the exact solution. In reality, there are a large variety of possible modes, and the details of any given mode depend sensitively on k_θ, θ_k, l, $\hat{s}$, and other parameters. We have not attempted to follow the details of the individual modes, but we expect that the theory is a fairly good representation of the average collective behavior (scalings, ordering, etc.) of the linear modes.

The modes considered here have several differences from those usually discussed[19,22] in the context of the toroidal η_i threshold. It would be premature to say here whether one solution is more correct than the other, since a different part of k_θ space has been considered [$k_\theta \rho_i \to 0$ in Ref. 19, while $k_\theta \rho_i \sim O(1)$ here], and also the present analysis applies only insofar as the WKB approach is valid. However, the previous picture would benefit from a derivation that reconciles poloidal localization with the $k_\parallel v_\parallel \ll \omega_{Di}$ expansion, as discussed in Sec. III A. One difference is the parallel structure of the modes, which usually is considered to be localized about $\hat{\theta} \sim 0$ with long parallel wavelength, and here is centered about any θ_k, with considerably shorter parallel wavelength $[qRk_\parallel \sim O(1/\sqrt{\epsilon_T})]$. A second difference is that here parallel sound wave destabilization dominates the effects of bad curvature. This leads to the result that unstable modes can be distributed over all poloidal locations, not just regions of unfavorable curvature (in fact, for high shear, regions with favorable curvature might be slightly preferred, since the lowest threshold occurs for $\theta_k = \pi$). A third difference is that here, parallel resonances dominate over drift resonances. While either resonance provides $\eta_c^{\text{tor}} \sim 1 + O(\epsilon_n)$, the difference has considerable impact on the nonlinear theory, where resonances provide the nonlinear saturation. In summary, the present analysis may be characterized as much closer to the slab picture, although significant differences exist, such as the ordering of ω_r and $k_\parallel$.

It is useful to note briefly what was gained from the detailed solution for $\hat{\phi}^{(0)}$ presented above. This can be done by comparing the results that would have been obtained from the more standard methods of Taylor expanding Q about $\hat{\theta} = 0$, or approximating the potential as a quadratic between any two turning points. In the present problem, the simpler approaches would imply that the mode is centered about $\hat{\theta} = 0$, or about any of the potential wells of $\sin\hat{\theta}$, whereas the detailed analysis shows that the only allowable modes are centered around $\hat{\theta} \sim \theta_k$. This has the important effect of minimizing the local $k_r(\hat{\theta})$, which is important for determining the radial correlation length. Also, the simpler approaches would always give a mode width of about π, whereas the present analysis shows that $\Delta_{\hat{\theta}}$ decreases with increasing shear ($\hat{s}$), again with an impact on the resulting radial correlation length. These differences in the lowest-order mode structure in turn affect γ, the nonlinear saturation, and the transport.

We now comment on the validity of various approximations used in this section. First, the validity of the curvature approximation can be checked by noting that, with the eventual ordering of the mode, the velocity integral could also be

performed by expanding the denominator of the integrand in Eq. (5) for $\omega_{Di} \ll \omega - k_\parallel v_\parallel$. (For $|\hat{\theta} - \theta_k| > 1/\sqrt{\epsilon_T}$, $\omega_{Di} > k_\parallel v_\parallel$, making this expansion invalid, but this occurs well outside the limits of the mode, which has $|\hat{\theta} - \theta_k| \lesssim 1/\hat{s} \sim 1$.) This leads to an equation similar to Eq. (9), but the curvature approximation is preferred because it avoids the need for such an *a priori* ordering assumption at this point. Second, the weak instability ordering that allows Eq. (9) to be divided into Eqs. (10) and (14) requires that $\gamma < \omega_r$, taking $\Omega_R \simeq 2\epsilon_n$, and Eq. (26) gives the requirement

$$\eta_i - \eta_{\text{thresh}}^{\text{tor}} < 2\epsilon_n \sqrt{(1 + 1/\tau)/\epsilon_T}. \tag{27}$$

Other restrictions of the theory include $k_\theta \gtrsim O(1)$, $\epsilon_T \ll 1$ (although $\epsilon_n \to \infty$ is permissible, with slight redefinitions of various parameters). Third, validity of the WKB approximation and the local treatment of $k_\parallel$ require that the scale length of $Q_R(\hat{\theta})$ (of order 1) is longer than that of $\hat{\phi}(\hat{\theta})$ (which from Eq. (22) is of order $\sqrt{\epsilon_T}$). Thus the WKB approximation applies in the limit $\epsilon_T \ll 1$. The analytical solution for $\phi^{(0)}$ and Ω_R has been tested with a shooting code solution of Eq. (10). Figure 1 shows a typical mode, and Fig. 2 shows Ω_R as a function of k_θ. It is found that the analytical solution describes well the average behavior in a gross sense (i.e., scalings, orders of magnitude, cutoff at low l, average mode width, $k_\parallel$, etc.), but the complicated behavior of the exact solution means that the details of a mode at a given $\mathbf{k}$ might deviate somewhat. Finally, it would be desirable to compare the analytical prediction of the growth rate with numerics, but this cannot be done with the simple shooting method used here. The difficulty lies in the dependence of γ on Im Z in Eqs. (15) and (16), which in turn varies with $k_\parallel/|k_\parallel|$. This term is easily handled in the WKB approximation (where $k_\parallel$ is treated as a number), but presents difficulty in the context of a shooting code (where the operator $\nabla_\parallel$ is used instead). It should be possible to check the existence and growth of these modes with existing gyrokinetic codes.[19,31-33] However, such studies have concentrated either on the $l = 0$ branch[31] or the $k_\theta \rho_i \ll 1$ limit[33] of the mode. The modes examined here, with $l \sim R/L_n$ and $k_\theta \rho_i \gtrsim 1$, have apparently not been addressed, although the present study suggests that they can be quite unstable near threshold. Furthermore, these modes are interesting since they provide a paradigm to study the effects of nonlinear Landau damping on the toroidal η_i mode, which may be important for all branches of the mode.

IV. NONLINEAR THEORY

In this section we examine the nonlinear saturation of the linearly unstable modes just above the threshold, the linear properties of which are described in Sec. III B 3 above. A weak turbulence expansion[15] is used to derive the wave kinetic equation, which is then solved to yield the turbulent spectrum. This expansion requires that the nonlinear terms be less than the dominant linear term, which is equivalent to the threshold ordering already employed in the linear theory ($\gamma < \omega_r$). To facilitate this analysis, we use a local analysis in this section, whereby $k_\parallel$ is treated as a number in the wave kinetic equation [although the results from the normal mode analysis regarding the structure of $\hat{\phi}(\hat{\theta})$ are retained].

Application of the weak turbulence expansion to Eq. (3) proceeds by the same method as described in Ref. 14, and is not repeated here. To lowest order, this expansion yields Eq. (10) describing the linear mode structure and frequency, and to next order it yields the wave kinetic equation, which describes the evolution of the spectrum due to linear instability and also due to two nonlinear processes.[14] The first nonlinear process is three wave resonance, which is negligible since wave triplets that obey both $\mathbf{k} = \mathbf{k}' + \mathbf{k}''$ and $\omega_k = \omega_{k'} + \omega_{k''}$ are rare (due to the low level of frequency broadening in the weak turbulence regime combined with the strong dispersion of ω_r). The second saturation process is ion Compton scattering (which occurs when an ion resonates with the beat wave between two normal modes), which can be expected to accompany the presence of strong *linear* ion resonances. This is the dominant saturation mechanism for the threshold regime. To simplify notation, it is convenient to represent the nonlinear gyrokinetic equation, Eq. (3), as

$$-iL_{1,k}(\omega_k)\hat{h}_k - iL_{2,k}(\omega_k)\hat{\phi}_k = \sum_{p',p''} \sum_{n'} \int dk'_r\, C_{k',k''} \hat{\phi}_{k'} \hat{h}_{k''},$$

where the L represents the linear coefficients and the C represents the nonlinear coupling coefficient. With this, the wave kinetic equation (less the three wave resonance terms) can be written locally as

$$\frac{1}{2} \frac{\partial \operatorname{Re} \epsilon_k}{\partial \omega_r} \frac{\partial}{\partial t} |\hat{\phi}_k^2(\hat{\theta})| = -\operatorname{Im} \epsilon_k(\omega_r) |\hat{\phi}_k^2(\hat{\theta})| - \operatorname{Im} \sum_{n'} \int dk'_r\, \epsilon^{(3)}_{k',-k',k}(\omega_r) \times |\hat{\phi}_{k'}^2(\hat{\theta})| |\hat{\phi}_k^2(\hat{\theta})|, \tag{28}$$

where ϵ_k is the linear dielectric function given by Eq. (7),

$$\epsilon^{(3)}_{k',-k',k} = \frac{1}{2} \int d^3v \frac{J_0(k_\perp v_\perp) L_{2,k}(\omega_k) C_{k',k''} C_{-k',k}}{L_{1,k}(\omega_k)^2 L_{1,-k''}(-\omega_{k''})}, \tag{29}$$

$\omega_{k''} \equiv \omega_k - \omega_{k'}$ (not ω of the beat wave), $\mathbf{k}'' \equiv \mathbf{k} - \mathbf{k}'$ and ϵ_k is given by Eq. (8). The coupling of p is negligible for $\hat{s} > 1/\pi$ (since the quasimodes have width $\Delta_{\hat{\theta}} \lesssim 2/\hat{s}$), and has been left out of Eq. (28) (although the results would probably not change much otherwise). Also, there is a term in $\epsilon^{(3)}$ that has canceled under $\Sigma_{k'}$ by symmetry. Taking $\int_{-\infty}^{\infty} d\hat{\theta}$ of Eq. (28) reproduces Eq. (16) for the linear growth rate (with an additional nonlinear term). Here, we neglect this averaging process for simplicity, using instead quantities which reflect average behavior across the width of $\hat{\phi}_k$. Consistent with this approach, ϵ_k will be kept in the local form given by Eq. (8).

We next focus on reducing $\epsilon^{(3)}$ to a more tractable form. The calculation is facilitated by the fact that the ω_{Di} terms give only higher-order contributions to resonances, given the ordering of the linear theory. Thus, taking $L_{1,k}(\omega_k) \to \omega_k - k_\parallel v_\parallel$ for the lowest-order contribution to

the resonance allows the denominator in Eq. (29) to be written as the sums of single resonances

$$\frac{1}{L_{1,\mathbf{k}}(\omega_{\mathbf{k}})^2 L_{1,-\mathbf{k}'}(-\omega_{\mathbf{k}'})}$$

$$= \frac{1}{(\omega_{\mathbf{k}} k_\parallel' - \omega_{\mathbf{k}'} k_\parallel)^2}\left(\frac{k_\parallel''^2}{L_{1,\mathbf{k}'}(\omega_{\mathbf{k}'})} - \frac{k_\parallel k_\parallel''}{L_{1,\mathbf{k}}(\omega_{\mathbf{k}})} - \frac{\omega_{\mathbf{k}} k_\parallel' - \omega_{\mathbf{k}'} k_\parallel}{\omega_{\mathbf{k}}} \frac{\partial}{\partial\delta} \frac{k_\parallel}{L_{1,\mathbf{k}}(\delta\omega_{\mathbf{k}})}\bigg|_{\delta=1}\right).$$

Applying this to Eq. (29) yields

$$\begin{aligned}
\mathrm{Im}\,\epsilon^{(3)}_{\mathbf{k}',-\mathbf{k}',\mathbf{k}} &= -\omega_{*i}(2\pi\hat{s}k_\theta k_\theta')^2 \frac{(\theta_{\mathbf{k}}-\theta_{\mathbf{k}'})^2}{(\omega_{\mathbf{k}} k_\parallel' - \omega_{\mathbf{k}'} k_\parallel)^2}\left[1 - \frac{3}{2}\eta_i - \eta_i\left(\frac{\partial}{\partial\alpha} + \frac{\partial}{\partial\beta}\right)\right] G\left(\frac{b_\theta}{\beta}, \frac{b_\theta'}{\beta}\right)\bigg|_{\beta=1} \\
&\quad \times \mathrm{Im}\,\frac{1}{\sqrt{\pi}}\int_{-\infty}^{\infty} dv_\parallel\, e^{-\alpha v_\parallel^2/2}\left(\frac{k_\parallel''^2}{L_{1,\mathbf{k}''}(\omega_{\mathbf{k}''})} - \frac{k_\parallel k_\parallel''}{L_{1,\mathbf{k}}(\omega_{\mathbf{k}})} - \frac{\omega_{\mathbf{k}} k_\parallel' - \omega_{\mathbf{k}'} k_\parallel}{\omega_{\mathbf{k}}} \frac{\partial}{\partial\delta}\frac{k_\parallel}{L_{1,\mathbf{k}}(\delta\omega_{\mathbf{k}})}\bigg|_{\delta=1}\right) \\
&= -\sqrt{\pi}\omega_{*i}(2\pi\hat{s}k_\theta k_\theta')^2 \frac{(\theta_{\mathbf{k}}-\theta_{\mathbf{k}'})^2}{(\omega_{\mathbf{k}} k_\parallel' - \omega_{\mathbf{k}'} k_\parallel)^2}\left[\eta_i G'(b_\theta, b_\theta') - G(b_\theta, b_\theta')\right] k_\parallel''\left(\frac{k_\parallel''}{|k_\parallel''|} - \frac{k_\parallel}{|k_\parallel|}\right), \qquad (30)
\end{aligned}$$

where

$$G(b,b') = \int_0^\infty d(v^2) J_0^2(\sqrt{2b}\,v) J_0^2(\sqrt{2b'}v)\exp(-v^2),$$

$$G'(b,b') = \left(\frac{3}{2} + \frac{\partial}{\partial\beta}\right)\frac{1}{\beta} G\left(\frac{b}{\beta}, \frac{b'}{\beta}\right)\bigg|_{\beta=1},$$

and any terms of relative order $\sqrt{\epsilon_T}$ (by the linear ordering) have been dropped. In evaluating the contribution from parallel resonances, analytic continuation has been applied (yielding terms like $k_\parallel/|k_\parallel|$), which changes the symmetry properties of $\epsilon^{(3)}$, and has an impact on the nature of the turbulent energy transfer (discussed near the end of this section).

The wave kinetic equation, Eq. (28), can now be written as

$$\frac{1}{2}\frac{\partial}{\partial t}|\hat{\phi}_{\mathbf{k}}^2(\hat{\theta})| = (\gamma_{\mathbf{k}} + \gamma_{\mathbf{k}}^{\mathrm{NL}})|\hat{\phi}_{\mathbf{k}}^2(\hat{\theta})|. \qquad (31)$$

Here, the linear growth rate $\gamma_{\mathbf{k}}$ can be obtained by using the local form of $\epsilon_{\mathbf{k}}$, and is given by

$$\gamma_{\mathbf{k}} = (\sqrt{2\pi}|k_\parallel|/\eta_i\eta_c)(\eta_i - \eta_c^{\mathrm{tor}}), \qquad (32)$$

where $\eta_c(1 - \Omega_R + \eta_i\zeta^2) \simeq \eta_c^{\mathrm{tor}}$ has been used. (Note that $\gamma_{\mathbf{k}}$ does not increase indefinitely with $k_\parallel$, since η_c^{tor} has implicit $k_\parallel$ dependence.) The nonlinear growth can be written by inserting $\epsilon^{(3)}$ into Eq. (28), and is given by

$$\begin{aligned}
\gamma_{\mathbf{k}}^{\mathrm{NL}} \simeq &-\frac{8\pi^{5/2}(\hat{s}k_\theta)^2}{\Gamma_0\eta_i}\int dk_r' \sum_{k_\theta'} \frac{k_\theta'^2}{k_\parallel'^2}\frac{(\theta_{\mathbf{k}}-\theta_{\mathbf{k}'})^2}{(\zeta-\zeta')^2} \\
&\times \left[\eta_i G'(b_\theta, b_\theta') - G(b_\theta, b_\theta')\right] \\
&\times |k_\parallel''|\Theta(-k_\parallel'' k_\parallel)|\hat{\phi}_{\mathbf{k}'}^2(\hat{\theta})|, \qquad (33)
\end{aligned}$$

where Θ is the Heaviside step function and $\zeta' \equiv \omega_{\mathbf{k}'}/\sqrt{2}k_\parallel'$.

In the saturated state, $\partial|\hat{\phi}^2|/\partial t \to 0$, and Eq. (31) becomes $\gamma_{\mathbf{k}} + \gamma_{\mathbf{k}}^{\mathrm{NL}} = 0$, giving an equation for the saturated turbulent spectrum. In order to solve this, it is useful to approximate the spectral sums (in n' and k_r') as integrals. Making use of the Heaviside step function, the symmetry of the summand upon reflection in $k_\parallel$, $k_\parallel'$, and $k_\parallel''$, and the fact that $k_\parallel$ is an increasing function of n, the n summation can be approximated as

$$\sum_{n'=-\infty}^{\infty} \Theta(-k_\parallel k_\parallel'') \to 2\sum_{n''=0}^{\infty} \to \frac{2r}{q}\int_0^\infty dk_\theta''.$$

The k_r' sum can be transformed into an integral over $\theta_{\mathbf{k}}$ by recalling that $k_r' = \hat{s}k_\theta\theta_{\mathbf{k}'}$, and the limits of this integral come from the fact that for $|\theta_{\mathbf{k}} - \theta_{\mathbf{k}'}| \gtrsim 1/\hat{s}$ the modes $\hat{\phi}_{\mathbf{k}}$ and $\hat{\phi}_{\mathbf{k}'}$ do not overlap (since the modes have width $\Delta_{\hat{\theta}} \simeq 1/\hat{s}$ in ballooning space), which allows

$$\int_{-\infty}^{\infty} dk_r' |\hat{\phi}_{\mathbf{k}'}^2(\hat{\theta})|(\cdots) \to k_\theta\hat{s}\int_{-1/\hat{s}}^{1/\hat{s}} d\theta_{\mathbf{k}}'' |\hat{\phi}_{\mathbf{k}'}^2|(\cdots),$$

where $\theta_{\mathbf{k}}'' \equiv \theta_{\mathbf{k}} - \theta_{\mathbf{k}}'$, and $|\hat{\phi}_{\mathbf{k}'}^2| \equiv |\hat{\phi}_{\mathbf{k}'}^2(\theta_{\mathbf{k}'})|$. With this, the balance between linear growth and nonlinear damping may be written as the following integral equation:

$$\begin{aligned}
\eta_i - \eta_c^{\mathrm{tor}} = &\frac{2\sqrt{2}(2\pi)^2\hat{s}^3\eta_c}{\Gamma_0}\int_{-1/\hat{s}}^{1/\hat{s}} d\theta_{\mathbf{k}}'' \int_0^\infty dk_\theta'' \frac{k_\theta^2 k_\theta'^3 |k_\parallel''|}{|k_\parallel| k_\parallel'^2} \\
&\times \frac{\theta_{\mathbf{k}}''^2}{\zeta''^2}\left[\eta_i G'(b_\theta, b_\theta') - G(b_\theta, b_\theta')\right]|\hat{\phi}_{\mathbf{k}'}|^2, \qquad (34)
\end{aligned}$$

where $\zeta'' \equiv \zeta - \zeta'$ (not ζ of the beat mode)! Concentrating first on the k_θ'' integral, the equation can be reduced by noting that the contribution from the $k_\theta'' \to 0$ end of the integration is larger than that from the $k_\theta'' \to \infty$ end. This can be seen by recalling from the linear theory that $k_\parallel \propto \sqrt{k_\theta}$, $\omega_{\mathbf{k}} \propto k_\theta$, and $\zeta \propto \sqrt{k_\theta}$, with $\theta_{\mathbf{k}}$ dependences present but weaker. Furthermore, one can show that G and G' are proportional to $1/k_\theta k_\theta'$. With all this, it is easy to verify that as $k_\theta'' \to 0$ (and $k_\theta' \to k_\theta$, which is fixed) the integrand in the above varies as

$$\lim_{k_\theta'' \to 0} [\text{integrand in Eq. (34)}] \propto \frac{k_\theta''}{\left[k_\theta''(\partial\zeta/\partial k_\theta) + \theta_{\mathbf{k}''}(\partial\zeta/\partial\theta_{\mathbf{k}})\right]^2},$$

which demonstrates that there is a logarithmic divergence resolved only by the weak dependence of ζ on $\theta_{\mathbf{k}}$. On the other hand, for $k''_\theta \to \infty$, $k'_\theta \to -k''_\theta$, and we have

$$\lim_{k''_\theta \to \infty} [\text{integrand in Eq. (34)}] \propto |\hat{\phi}_{\mathbf{k}''}|^2/\sqrt{k''_\theta},$$

which converges well if the spectrum vanishes faster than $1/\sqrt{k_\theta}$ (it will be seen *a posteriori* that the spectrum vanishes as $1/k_\theta^2$). Thus the k''_θ integral can be performed by keeping only the dominant contribution from the lower limit, for which $k'_\theta \simeq k_\theta$, and Eq. (34) becomes

$$\eta_i - \eta_c^{\text{tor}} = \frac{2\sqrt{2}(2\pi)^2 \hat{s}^3 \eta_c}{\Gamma_0} \frac{k_\theta^5}{k_\parallel^3} \times [\eta_i G'(b_\theta, b_\theta) - G(b_\theta, b_\theta)] |\hat{\phi}_{\mathbf{k}}|^2 \times \int_0 dk''_\theta \int_{-1/\hat{s}}^{1/\hat{s}} d\theta''_{\mathbf{k}} \frac{|k''_\parallel| \theta''^2_{\mathbf{k}}}{\zeta''^2}. \tag{35}$$

The $\theta''_{\mathbf{k}}$ integral is performed by keeping only the $\theta''^2_{\mathbf{k}}$ dependence in the integrand (thereby taking advantage of the relative flatness of the spectrum in $\theta_{\mathbf{k}}$). This leads to the following spectrum:[28]

$$|\hat{\phi}_{\mathbf{k}}|^2 \simeq \frac{1}{(2\pi)^2} \frac{q}{r} \frac{\eta_i - \eta_c^{\text{tor}}(\mathbf{k})}{|\ln \partial\zeta/\partial\theta_{\mathbf{k}}|} \frac{1}{R^2 k_\theta^3}, \tag{36}$$

and $|\hat{\phi}^2_{\mathbf{k}}| = 0$ in regions of $\mathbf{k}$ space, where $\eta_i \leqslant \eta_c^{\text{tor}}(\mathbf{k})$. The logarithmic term in the denominator represents a correction of order unity, and since $\partial\zeta/\partial\theta_{\mathbf{k}}$ is not calculated in this theory, we shall neglect it.

It is useful to convert the quasimode spectrum of Eq. (36) into a Fourier spectrum, since this is what would be measured experimentally. The primary difference between the two is the radial wave number, which is constant for a Fourier mode, but varies along the parallel direction of a quasimode. The relation between the two spectra can be obtained from the Fourier transform of Eq. (1), which produces

$$\tilde{\phi}_{\mathbf{k}} = \int_{-\infty}^{\infty} d\hat{\theta}\, e^{i(m - nq)\hat{\theta}} \hat{\phi}_{n, k + k_\theta \hat{s}\hat{\theta}}(\hat{\theta}) \simeq \hat{\phi}_{\mathbf{k}} \Theta(|k_\theta| - |k|) \delta_{m - nq, \hat{k}_{\hat{\theta}}}, \tag{37}$$

where k is the radial wave number of the Fourier modes, $\hat{k}_{\hat{\theta}}$ is the parallel wave number in terms of the ballooning coordinate, Θ is the Heaviside step function, and in the second step of Eq. (22) has been used for $\hat{\phi}(\hat{\theta})$. The Kronecker delta function describes the localization of the real space fluctuations to the rational surfaces. In a more careful treatment, the parallel wave number $\hat{k}_{\hat{\theta}}$ would be a wave packet, and the delta function would become an envelope describing the radial width of a fluctuation. Equation (37) shows that the Fourier spectrum is similar to the quasimode spectrum in k_θ, and with a (roughly) flat spectrum of radial wavelengths of width k_θ. Note that a more complete theory would predict a radial envelope for $\hat{\phi}$, giving the radial Fourier spectrum a cutoff as $k \to 0$.

Compared with the mixing length level of $\tilde{\phi}$ generally invoked for strong fluid toroidal η_i turbulence,[19,29] Eqs. (36) and (37) are smaller by roughly a factor of $L_T/R \ll 1$, implying that nonlinear ion resonances are a strong damping mechanism for toroidal η_i turbulence. However, the difference in saturation levels here is not as pronounced as in the slab model, where a factor of $(L_T/R)^2$ was found.[14] The difference from the slab model seems not to arise from any fundamental difference in the physics, but rather from the different linear ordering of ω_r and $k_\parallel$ in the two models. These points are discussed further at the end of Sec. V.

It appears that this nonlinear saturation process (involving two waves and a particle) transfers energy directly from the spectrum to the particle distribution, without conserving turbulence energy. This can be seen by noting the following points from Eq. (30) (which is not approximated beyond application of the weak turbulence expansion, the eikonal approach, and the ordering from the linear theory).

(1) The nonlinear growth of $\hat{\phi}_{\mathbf{k}}$ comes only from interaction with the $\hat{\phi}_{\mathbf{k}'}$ that have $k'_\parallel$ larger than $k_\parallel$ (owing to the presence of the Heaviside step function, with $k''_\parallel \equiv k_\parallel - k'_\parallel$).

(2) The nonlinear growth rate is negative definite for $\eta_i G'_{k,k'} > G_{k,k'}$ (true whenever the linear instability criterion is satisfied).

Point (1) implies that in the nonlinear interaction between $\hat{\phi}_{\mathbf{k}}$ and $\hat{\phi}_{\mathbf{k}'}$ only the former changes energy, and the only place for the energy to go is the distribution function. Furthermore, $\phi_{\mathbf{k}}$ must be *damped* by this process, by point (2) above. Thus the nonlinear process transfers energy from the mode with lower $k_\parallel$ to the resonant ions, and the second mode plays the role of a nonlinear catalyst that neither gains nor loses energy. This means that an η_i instability saturated by nonlinear Landau damping does not require a part of $\mathbf{k}$ space where the modes are linearly stable; the nonlinear process itself provides an energy sink. It appears that this picture of nonlinear Landau damping also applies to the slab limit of the η_i instability, although a previous work[14] did not uncover this fact, because of the less detailed treatment of the nonlinear scattering term. Specifically, the previous work did not apply analytic continuation to the resonant denominator, Eq. (29), which leads eventually to the Heaviside step function in Eq. (33) and has a significant impact on the symmetry properties with respect to $\mathbf{k}$ and $\mathbf{k}'$.

It is well known that drift waves can also saturate by nonlinear wave–particle interaction,[15,33] except that it is generally found that this process transfers energy to waves, not to the particle distribution. The underlying difference can be seen from the relative ordering of the phase and thermal velocities, which leads to an adiabatic constraint for drift waves, but not for η_i modes. For drift waves, the linear time scale is characterized by $\omega \gg k_\parallel v_i$, while nonlinear wave–particle interaction requires $\omega - \omega' = (k_\parallel - k'_\parallel) v_i \sim k_\parallel v_i$. The nonlinear interaction is thus *slow* relative to the linear time scales ($|\omega| \gg |\omega - \omega'|$), and can be regarded as an adiabatic perturbation on the waves, which conserves wave action density through the well known Manley–Rowe relations.[15] However, in the case of η_i modes near the threshold $\omega \lesssim k_\parallel v_i$, and so there is no such adiabatic constraint on energy transfer, thus allowing the particles to acquire a large part of the energy, as described in the preceding paragraph.

(This does not explain why the ions must receive the energy; only how they can.) For this reason, the term "ion Compton scattering" seems more appropriate for the drift wave saturation process (suggesting elastic energy transfer from incoming to outgoing waves), and "nonlinear Landau damping" seems more appropriate for the η_i saturation process described here (suggesting direct transfer of wave energy to the distribution function).

V. TRANSPORT

Having obtained the saturated turbulent spectrum, the associated ion thermal transport due to $\mathbf{E}\times\mathbf{B}$ convection may now be calculated. This simplified model does not allow calculation of particle or electron heat fluxes (since electrons have been taken as adiabatic), or of momentum flux (since there is no equilibrium shear flow), but these phenomena may be considered as secondary to the basic dynamics of η_i turbulence, which concerns relaxation of the ion temperature gradient.

Before proceeding with the calculation, it is important to discuss the diffusive nature of the transport. This is an issue because the radial width of the quasimodes is very large[24,25] (in fact, infinite to the order considered here), and thus each individual linear mode represents a broad convective cell, implying nondiffusive transport. The variation of the local $k_r(\hat{\theta})$ of a quasimode does not change the situation, since this merely represents the fact that the convective cell twists as it follows the sheared field lines. What does change the situation is the superposition of another mode with a different k_r, i.e., one centered farther down the field line with a twist relative to the first mode. The beat mode between these two (and ultimately many modes) has an oscillatory radial structure, thus breaking the smooth convective pattern of any one mode. Thus the k_r spectrum (generally not considered in toroidal theories, which tend to assume a single maximally unstable k_r) is important for giving radial structure to the fluctuations, decorrelating a fluctuation in a radial distance of $1/\hat{s}k_\theta\Delta_{\hat{\theta}}\sim\rho_i$ (where $\Delta_{\hat{\theta}}$ is the parallel width of a quasimode). This reconciles diffusive transport with the broad radial width of the linear modes. The situation is analogous to homogeneous Navier–Stokes turbulence, where a given plane wave extends over the entire domain of the fluid; but this long range correlation is broken nonlinearly by the random superposition of many plane waves of different $\mathbf{k}$.

The radial ion thermal flux q_i from the turbulent $\mathbf{E}\times\mathbf{B}$ drift is given by

$$q_i=\frac{c}{B}\int d^3v\,\frac{mv^2}{2}\,\langle\tilde{h}(\mathbf{x})\nabla_\theta\tilde{\phi}(\mathbf{x})\rangle, \tag{38}$$

where $\langle\cdots\rangle$ represents an average over the fast fluctuations. Introducing the ballooning transform via Eq. (2), and carrying out the averages, we find

$$q_i=(2\pi)^2\,\mathrm{Re}\int d^3v\,\frac{mv^2}{2}\int dk_r\sum_{n,p,p'}\frac{1}{2\pi}\times\int_0^{2\pi}d\theta\,e^{-2\pi i n q(p-p')}(-ik_\theta)J_0(k_\perp v_\perp)\times\hat{\phi}_{\mathbf{k}}(\theta+2\pi p)\hat{h}_{-\mathbf{k}}(\theta+2\pi p'). \tag{39}$$

As in the nonlinear theory, the p and p' sums can be neglected for $\hat{s}\gtrsim 1/\pi$ (with assumedly not much difference; even when this condition is not met), and the θ average neglected since θ dependencies of the integrand are higher order. In the weak turbulence regime, $\hat{h}$ is dominated by the quasilinear contribution, and so substituting $\hat{h}_{-\mathbf{k}}$ from the linearized gyrokinetic equation and performing the velocity space integration, after some calculation, produces

$$q_i=-\frac{(2\pi)^2 m_i}{L_n}\int dk_r\sum_n\frac{k_\theta^2\Gamma_0}{|k_\parallel|}|\hat{\phi}_{\mathbf{k}}|^2, \tag{40}$$

where the approximation $\Gamma_1\simeq\Gamma_0\simeq 1/\sqrt{2\pi b_\theta}$ has been applied (valid over the excited part of the spectrum, which has $b_\theta\gtrsim 1$). Inserting the spectrum from Eq. (36), and $k_\parallel$ from the linear theory, we obtain

$$q_i\simeq -m_i\sqrt{1+\frac{1}{\tau}}(\eta_i-\eta_{\mathrm{thresh}}^{\mathrm{tor}})\,\frac{\sqrt{L_T}}{R^{3/2}L_n}, \tag{41}$$

or an ion thermal conductivity of

$$\chi_i\equiv\frac{-q_i}{\nabla_r T_i}=\sqrt{1+\frac{1}{\tau}}\left(\frac{\eta_i-\eta_{\mathrm{th}}^{\mathrm{tor}}}{\eta_i}\right)\frac{\sqrt{L_T}}{R^{3/2}}. \tag{42}$$

Compared with the mixing length level often invoked[19,29] for strong toroidal η_i turbulence, the above χ_i is smaller by a factor of about L_T/R (as expected from the reduction of spectral amplitude through nonlinear Landau damping). Even with this reduction, χ_i is in the range of experimental values.[34] This contrasts with a previous finding in the slab theory that Compton scattering reduces χ_i by a factor of about $(L_T/R)^2$, making it far too low to contribute to tokamak transport (see the next paragraph for a further discussion of this). In the toroidal theory, it is quite possible that the weak turbulence χ_i is large enough to give substantial transport in tokamaks.

It is useful to devise a rule of thumb for estimating χ_i on the basis of the linear theory, since the usual mixing length estimate clearly does not approximate Eq. (42) well (nor is it expected to, since it is based on orderings from fluid strong turbulence). This can be done by first estimating the saturated fluctuation level from Eqs. (31) and (33), which produces

$$\sum_{\mathbf{k}'}|\hat{\phi}_{\mathbf{k}'}^2|\simeq\frac{\zeta^2 k_\parallel\gamma_{\mathbf{k}}}{\eta_i k_\theta^2 k_r^2\Gamma_0}, \tag{43}$$

where approximations such as $\zeta-\zeta'\sim\zeta$ have been made, which can be expected to preserve the scalings, if not the exact numerical coefficients. Inserting Eq. (43) into the quasilinear formula, Eq. (40), gives the estimate

$$\chi_i\simeq\zeta^2\gamma/k_r^2. \tag{44}$$

This estimate accounts for the different kinetic reduction factors predicted by the slab and toroidal theories, where $\zeta^2\sim(L_T/L_s)^2$ and $\zeta^2\sim L_T/R$, respectively. It is not clear how general this formula is, since it is partly based on the linear ordering and weak turbulence expansion specific to the present theory. Equation (44) does, however, make a smooth transition to the usual mixing length estimate, and one might hypothesize that $\chi_i\simeq\gamma/k_r^2$ applies when $\zeta>1$

(fluid behavior), and is replaced by Eq. (44) when $\zeta < 1$ (kinetic behavior). It would be interesting to study the generality of this prescription, but this is beyond the scope of the present work.

VI. CONCLUSIONS

In this work we have examined the linear and nonlinear dynamics of the toroidal η_i mode near the threshold of instability, and the resulting transport. Results indicate that inclusion of the parallel dynamics of toroidal η_i modes can produce a threshold regime that is more similar to that of the slab η_i mode than generally thought. (It is important to note that modes with $k_\theta \rho_i \gtrsim 1$ are considered here, in contrast to the more usual $k_\theta \rho_i \ll 1$ assumption.) Linear stability is determined primarily by the balance of sound wave destabilization and damping from transit resonances ($\omega \simeq k_\parallel v_\parallel$), with smaller toroidal corrections, yielding a threshold that varies as $\eta_c^{\rm tor} = \eta_c^{\rm slab} + O(\epsilon_n)$. Note that neglecting $k_\parallel$ produces a similar threshold,[19] but predicts entirely different dynamics from those given here, which is especially important for the nonlinear dynamics and transport. Nonlinear saturation is provided by nonlinear Landau damping, and the resulting saturated fluctuations are smaller than the mixing length level[29] by a factor of approximately L_T/R. The associated ion thermal transport is reduced by a similar factor, but is still large enough to cause significant transport on tokamaks. Results indicate that $\chi \simeq \zeta^2 \gamma / k_r^2$ is possibly a replacement for the more usual $\chi = \gamma / k_\perp^2$ in situations where the instability is saturated by nonlinear Landau damping.

As η_i rises above this weak turbulence regime (where $\zeta \sim \sqrt{\epsilon_T}$), resonances will continue to be important until $\zeta \gtrsim 1$. Above some value of η_i (not addressed here), fluidlike modes begin to emerge,[17,18] for which ion resonances can be expected to be less important. However, the higher l eigenmodes (which are often more unstable) are generally more susceptible to resonance (since they have higher $k_\parallel$), and so it is possible that the transport from η_i turbulence is sensitive to the effects of nonlinear Landau damping at all values of η_i. It is also possible that nonlinear resonances persist even when linear resonances become unimportant, as in the case of drift waves. Given that kinetic saturation can quite clearly give important corrections (orders of magnitude) to the transport, and that it is ignored in all theories which invoke either fluid assumptions or mixing length assumptions, one might conclude that assessment of this effect is one of the major uncertainties facing reliable predictions from η_i mode theories.

It is desirable to compare the ion thermal conductivity given by Eq. (42) with experiments. The restriction $\eta_i - \eta_c^{\rm tor} \lesssim O(L_n/\sqrt{RL_T})$ means that experimental agreement is not expected over all parameter regimes, but it is possible that there will be restricted agreement in regions where ∇T_i is near the threshold. Possibly an experimental test of the present theory is to see whether Eq. (42) serves as a *lower limit* for the experimental χ_i [since the true χ_i can be expected to exceed Eq. (42) for η_i above the weak turbulence regime]. Note that although this weak turbulence theory is formally analyzed for narrow band turbulence (dominated by the linear dispersion relation), in practice such turbulence would be indistinguishable from broadband turbulence, due to the complicated nature of the linear dispersion relation (for example, see Fig. 2).

There are several basic issues addressed in this paper which could be useful in contexts beyond the present regime. First, the linear eigenmode solution (described in Sec. III B 1 and the Appendix) is apparently a new method of solving mode equations that can arise in toroidal geometry, wherein the mode near $\hat{\theta} = \theta_k$ is matched asymptotically to the Bloch eigenfunctions. The resulting Bohr–Sommerfeld phase quantization condition, Eq. (12), can be applied to any situation where the potential asymptotically approaches a periodic function. Compared with the more usual method of expanding the potential around some local minimum, this method can give significant corrections to the width and number of possible modes. (For example, in this work important corrections to the shear scaling are obtained.) A second observation here is that nonlinear Landau damping can transfer energy directly to the ion distribution, not conserving wave energy. This nonconservative nonlinear energy transfer can provide some fairly counterintuitive phenomena, such as the possibility of a saturated spectrum that does not need to couple to stable modes. Other implications arise regarding the relative role of turbulence in heating versus transport, but this is beyond the scope of the present paper. Finally, the present prescription for reconciling of the broad radial extent of toroidally coupled eigenmodes with diffusive transport (described at the beginning of Sec. V) could have broad applications. This scenario can be extended from weak to strong turbulence if one allows that an arbitrary turbulent field in sheared toriodal geometry can be represented as a sum of quasimodes with approximately random phase. (That the ballooning transform is a legitimate integral transform of an arbitrary field with flutelike symmetry has been discussed by Hazeltine and Newcomb.[35]) If such quasimodes have a broad spectrum of θ_k then nonlinear beat waves will have a radial correlation width of $1/k_\theta \hat{s} \Delta_{\hat{\theta}}$, where $\Delta_{\hat{\theta}}$ is the width of the mode in the ballooning coordinate. Note that this same mixing length is often invoked for spectra that contain only a single θ_k (e.g., Ref. 20) in which case the mechanism for producing such a length from much broader quasimodes is unclear. Cowley[36] has considered the toroidal mixing length problem from a different viewpoint, and shown that a single linear "twisting mode" (here termed quasimode) can encounter a secondary instability, which shortens the otherwise broad radial correlation implied by toroidal coupling. However, the study did not address the correlation length of the complicated, strongly turbulent flow that follows the onset and saturation of the secondary instability. The present description can be applied to understand the mixing length in this regime.

The results of this paper suggest several possible directions for further study. The relation between the slablike mode examined here and the ballooninglike mode of Refs. 19 and 22 should be more clearly established. It would be useful to explore the kinetic strong turbulence regime that exists between the threshold and fluid regimes (probably requiring

particle simulations). An important line of work would be to combine the present results with those of the fluid regime to produce a prediction of χ_i valid for all η_i. A study of the basic nature of nonlinear Landau damping would be interesting, in order to understand better the result that drift waves are elastically scattered, while η_i modes damp directly to the ion distribution. Finally, it would be of interest to establish the degree of generality of the formula $\chi \simeq \zeta^2 \gamma / k_r^2$ for transport from modes that saturate via nonlinear Landau damping, as the validity of such a formula could render a difficult problem more assessible.

ACKNOWLEDGMENTS

The author is particularly indebted to J. W. Connor for many valuable conversations and for pointing out the Bloch eigenfunction solution for the asymptotic linear mode equation. T. S. Hahm and L. Chen have provided useful insight concerning the result that nonlinear Landau damping transfers energy directly to the ions. Several conversations with R. J. Hastie and F. Tibone are also gratefully acknowledged.

APPENDIX: PHASE QUANTIZATION FOR LINEAR MODES

In this appendix, the WKB approximation is used to find the solutions of Eq. (11),

$$\frac{\partial^2}{\partial \hat{\theta}^2} \hat{\phi}_k - (\mu \sin \hat{\theta}) \hat{\phi}_k = 0, \tag{A1}$$

which vanish for $\hat{\theta} \to \pm \infty$, and also the quantization condition required to connect the two vanishing solutions. Pure WKB solutions have the form

$$\hat{\phi}_{\pm} = \exp(\pm i w),$$

where $w = |\int_{\theta_T}^{\hat{\theta}} \sqrt{Q}\, d\hat{\theta}\,|$ and θ_T is the turning point nearest to $\hat{\theta}$. The complication arises because these generally will not vanish asymptotically, since such solutions acquire a component of the divergent branch at any of the infinity of turning points. Instead, the appropriate eigenstates are those for which

$$\begin{pmatrix} \hat{\phi}_a(\hat{\theta} + 2\pi) \\ \hat{\phi}_b(\hat{\theta} + 2\pi) \end{pmatrix} = \lambda \begin{pmatrix} \hat{\phi}_a(\hat{\theta}) \\ \hat{\phi}_b(\hat{\theta}) \end{pmatrix}, \tag{A2}$$

where $\hat{\phi}_{a,b}$ are any two linearly independent solutions of Eq. (A1). Such an eigenstate will repeat at every interval of 2π, each time acquiring a factor of λ. If $|\lambda| < 1$, then $\hat{\phi}$ will decrease with $\hat{\theta}$, and vice versa. This corresponds to the Bloch eigenmodes,[30] $\hat{\phi} = e^{\alpha \hat{\theta}} f(\hat{\theta})$, where $\alpha = \ln \lambda$ and f is a function of period 2π.

To find the appropriate eigenmodes with the WKB approximation, $\hat{\phi}(\hat{\theta})$ is expressed as a linear combination of the dominant and subdominant solutions,

$$\hat{\phi}(\hat{\theta}) = \hat{\phi}_s(\hat{\theta}) + \hat{\phi}_d(\hat{\theta}) \equiv (\Delta\hat{\theta}^j, \theta^j_T)_s \hat{\phi}^j_s + (\Delta\hat{\theta}^j, \theta^j_T)_d \hat{\phi}^j_d. \tag{A3}$$

Here, $\phi^j_{s,d}$ are the linear coefficients of the subdominant and dominant WKB basis functions, expressed in the notation of Heading,[37]

$$(\Delta\hat{\theta}^j, \theta^j_T)_{s,d} \equiv \exp\left(\pm i \int_{\theta^j_T}^{\hat{\theta}} \sqrt{Q}\, d\hat{\theta} \right),$$

where $\Delta\hat{\theta}^j \equiv \hat{\theta} - \theta^j_T$ is the parallel coordinate relative to θ^j_T, and $\theta^j_T \equiv \pi j$ are the turning points of $Q = -\mu \sin \hat{\theta}$. Since there are turning points at each interval of π, a given WKB basis function $(\Delta\hat{\theta}^j, \theta^j_T)_{s,d}$ is valid only in the interval $\Delta\hat{\theta}^j < \pi$, but after an interval of 2π it is possible to express the basis functions in terms of the $j+2$ turning point:

$$\begin{aligned} \hat{\phi}(\hat{\theta} + 2\pi) &= \hat{\phi}_s(\hat{\theta} + 2\pi) + \hat{\phi}_d(\hat{\theta} + 2\pi)(\Delta\hat{\theta}^{j+2}, \theta^{j+2}_T)_s \hat{\phi}^j_s \\ &\quad + (\Delta\hat{\theta}^{j+2}, \theta^{j+2}_T)_d \hat{\phi}^j_d. \end{aligned} \tag{A4}$$

By matching Eqs. (A3) and (A4) using the WKB connection rules, it is straightforward but tedious to show that for j even (denoted by $2j$), then the dominant and subdominant basis functions will become mixed in the following way:

$$\begin{pmatrix} \hat{\phi}_s(\hat{\theta} + 2\pi) \\ \hat{\phi}_d(\hat{\theta} + 2\pi) \end{pmatrix} = \begin{pmatrix} \cos R & \sin R \\ -\sin R & \cos R \end{pmatrix} \times \begin{pmatrix} e^{-R} & 0 \\ 0 & e^{R} \end{pmatrix} \begin{pmatrix} \hat{\phi}_s(\hat{\theta}) \\ \hat{\phi}_d(\hat{\theta}) \end{pmatrix}, \tag{A5}$$

where $R = \int_0^{\pi} \sqrt{\mu \sin \theta}\, d\theta \simeq 2.37\sqrt{\mu}$. Combining Eq. (A5) with the eigenvalue equation, (A2), gives the following eigenvalues for the Bloch functions:

$$\lambda_{\pm} = \cos R \cosh R \pm \sqrt{\cos^2 R \cosh^2 R - 1}. \tag{A6}$$

The corresponding coefficients of the Bloch eigenvectors are given by

$$\begin{pmatrix} \hat{\phi}^{2j}_s \\ \hat{\phi}^{2j}_d \end{pmatrix}_{\pm} = \text{const} \times \begin{pmatrix} \lambda_{\pm} - \cos R e^{-R} \\ \sin R e^{R} \end{pmatrix}. \tag{A7}$$

It is important to note that $\lambda_+ = 1/\lambda_-$, corresponding to one exponentially growing and one exponentially shrinking solution. For the case when basis functions are in terms of the *odd* turning points, Eq. (A5) changes slightly, and a similar analysis gives the same eigenvalues, but the corresponding eigenvectors become

$$\begin{pmatrix} \hat{\phi}^{2j+1}_s \\ \hat{\phi}^{2j+1}_d \end{pmatrix}_{\pm} = \text{const} \times \begin{pmatrix} \sin R e^{R} \\ \lambda_{\mp} - \cos R e^{-R} \end{pmatrix}. \tag{A8}$$

In the full normal mode problem of Eq. (7), there is a central potential bounded on either side by the asymptotic regions with the form of Eq. (A1). The boundaries of the central region can be defined as the two turning points $\theta_{\pm Tc}$, beyond which the potential function $Q(\hat{\theta})$ is sufficiently close to its asymptotic limit. For simplicity, we consider only the case for which there are no turning points within the central region, and for which immediately outside $\theta_{\pm Tc}$ are classically "forbidden" zones where $Q < 0$. (The general case is more complicated, but qualitatively not much different.) Considering the three zones (the potential well, and the potential hills immediately neighboring this), and matching derivatives and connection rules, it is straightforward to show that the central zone connects the two neighboring zones as follows:

$$\begin{pmatrix} \hat{\phi}_s \\ \hat{\phi}_d \end{pmatrix}_{\hat{\theta} > \theta_{+Tc}} = \begin{pmatrix} \sin S & \cos S \\ \cos S & -\sin S \end{pmatrix} \begin{pmatrix} \hat{\phi}_s \\ \hat{\phi}_d \end{pmatrix}_{\hat{\theta} < \theta_{-Tc}}, \tag{A9}$$

where $S = \int_{\theta_- Tc}^{\theta_+ Tc} \sqrt{Q}\, d\hat{\theta}$. The mode will vanish asymptotically if the lower (upper) solution is the negative (positive) eigenmode of Eq. (A7) [Eq. (A8)]. Putting these into Eq. (A9) shows that the condition for these two vanishing branches to be matched is $\sin S = 0$ or

$$\int_{\theta_- Tc}^{\theta_+ Tc} \sqrt{Q}\, d\hat{\theta} = l\pi, \tag{A10}$$

where $l = 0,1,\ldots$. Equation (A10) is the desired phase quantization condition. It is similar to the usual phase quantization condition connecting pure WKB basis functions, except that l replaces the usual $l + \frac{1}{2}$. The important information gained from this analysis is that a proper normal mode is located in the central region, and nowhere else.

[1] M. Greenwald, D. Gwinn, S. Milora, J. Parker, R. Parker, and S. Wolfe, in *Plasma Physics and Controlled Nuclear Fusion Research*, Proceedings of the 10th International Conference, London (IAEA, Vienna, 1984), Vol. I, p. 45.

[2] D. L. Brower, W. A. Peebles, S. K. Kim, N. C. Luhmann, Jr., W. M. Tang, and P. E. Phillips, Phys. Rev. Lett. **59**, 49 (1987).

[3] N. Mattor and P. H. Diamond, Phys. Fluids **31**, 1180 (1988).

[4] S. M. Wolfe, Bull. Am. Phys. Soc. **34**, 1913 (1989).

[5] M. C. Zarnstorff, N. L. Bretz, P. C. Efthimion, B. Grek, K. Hill, D. Johnson, D. Mansfield, D. McCune, D. K. Owens, H. Park, A. Ramsey, G. L. Schmidt, B. Stratton, E. Synakowski, and G. Taylor, in *17th European Conference on Controlled Fusion and Plasma Heating* (EPS, Petit-Lancy, Switzerland, 1990), Vol. I, p. 42.

[6] B. Balet, D. Bartlett, J. G. Cordey, C. Gowers, G. W. Hammett, M. v. Hellerman, J. O'Rourke, P. Morgan, P. Nielsen, G. Sadler, P. M. Stubberfield, and H. Weisen, in *17th European Conference on Controlled Fusion and Plasma Heating* (EPS, Petit-Lancy, Switzerland, 1990), Vol. I, p. 162.

[7] F. Tibone, G. Corrigan, and T. E. Stringer, in *17th European Conference on Controlled Fusion and Plasma Heating* (EPS, Petit-Lancy, Switzerland, 1990), Vol. II, p. 805.

[8] A. A. Galeev, V. N. Oraevskiĭ, and R. Z. Sagdeev, Sov. Phys. JETP **17**, 615 (1963).

[9] B. Coppi, M. N. Rosenbluth, and R. Z. Sagdeev, Phys. Fluids **10**, 582 (1967).

[10] B. B. Kadomtsev and O. P. Pogutse, in *Reviews of Plasma Physics*, edited by M. A. Leontovitch (Consultants Bureau, New York, 1970), Vol. 5, p. 249.

[11] G. S. Lee and P. H. Diamond, Phys. Fluids **29**, 3291 (1986).

[12] J. W. Connor, Nucl. Fusion **26**, 193 (1986).

[13] R. Sydora, T. S. Hahm, W. W. Lee, and J. M. Dawson, Phys. Rev. Lett. **64**, 2015 (1990).

[14] N. Mattor and P. H. Diamond, Phys. Fluids B **1**, 1980 (1989).

[15] R. Z. Sagdeev and A. A. Galeev, *Nonlinear Plasma Theory*, edited by T. M. O'Neil and D. L. Book (Benjamin, New York, 1969), pp. 89–117.

[16] J. W. Connor, R. J. Hastie, and J. B. Taylor, Proc. R. Soc. London **365**, 1 (1979).

[17] W. Horton, D.-I. Choi, and W. M. Tang, Phys. Fluids **24**, 1077 (1981).

[18] S. C. Guo, L. Chen, S. T. Tsai, and P. N. Guzdar, Plasma Phys. Controlled Fusion **31**, 423 (1989).

[19] F. Romanelli, Phys. Fluids B **1**, 1018 (1989).

[20] H. Biglari, P. H. Diamond, and M. N. Rosenbluth, Phys. Fluids B **1**, 109 (1989).

[21] P. N. Guzdar, L. Chen, W. M. Tang, and P. H. Rutherford, Phys. Fluids **26**, 673 (1983).

[22] P. W. Terry, W. Anderson, and W. Horton, Nucl. Fusion **22**, 487 (1982).

[23] A. Jarmén, P. Andersson, and J. Weiland, Nucl. Fusion **27**, 941 (1987).

[24] R. J. Hastie, K. W. Hesketh, and J. B. Taylor, Nucl. Fusion **19**, 1223 (1979).

[25] J. W. Connor and J. B. Taylor, Phys. Fluids **30**, 3180 (1987).

[26] A. Hirose and O. Ishihara, Nucl. Fusion **27**, 9 (1987).

[27] E. A. Frieman and L. Chen, Phys. Fluids **25**, 502 (1982).

[28] When comparing this with other theoretical spectra, one should keep in mind that $\int_{k_r}$ has been used here, instead of the more usual Σ_{k_r}. Use of the former over the latter introduces an extra factor of $1/k_\theta$ in the spectrum, Eq. (36).

[29] W. M. Tang, Nucl. Fusion **20**, 1605 (1986).

[30] C. Kittel, *Introduction to Solid State Physics* (Wiley, New York, 1976), 5th ed., pp. 190–195.

[31] G. Rewoldt and W. M. Tang, Phys. Fluids B **2**, 318 (1990).

[32] X. Q. Xu and M. N. Rosenbluth, Bull. Am. Phys. Soc. **35**, 2036 (1990).

[33] F. Y. Gang, P. H. Diamond, and M. N. Rosenbluth, Phys. Fluids B **3**, 68 (1991).

[34] F. Tibone (private communication).

[35] R. D. Hazeltine and W. A. Newcomb, Phys. Fluids B **2**, 7 (1990).

[36] S. C. Cowley, Bull. Am. Phys. Soc. **35**, 2080 (1990).

[37] J. Heading, *An Introduction to Phase Integral Methods* (Wiley, New York, 1962).